

The Relative Contributions of CYP3A4 and CYP3A5 to the Metabolism of Vinorelbine

Ariel R. Topletz, Ph.D., Jennifer B. Dennison, Ph.D., Robert J. Barbuch, Ph.D., Chad E. Hadden, Ph.D., Stephen D. Hall, Ph.D. and Jamie L. Renbarger, M.D., M.S.

Division of Clinical Pharmacology, Department of Medicine, Indiana University School of Medicine, Indianapolis, IN (ART, JBD, SDH, JLR); ¹Lilly Research Laboratories, Eli Lilly and Company, Indianapolis, IN (RJB, CEH, SDH)

Running Title: Vinorelbine metabolism by CYP3A

Corresponding Author:

Jamie L. Renbarger, MD, MS

Division of Clinical Pharmacology

Indiana University School of Medicine

1001 W. 10th Street, Rm 7123

Indianapolis, IN 46202

Phone: 317-630-8795

Fax: 317-278-0616

Email: jarenbar@iupui.edu

Pages: 27

Tables: 3

Figures: 6

References: 28

No. Words in Abstract: 228

No. Words in Introduction: 679

No. Words in Discussion: 1255

Non standard abbreviations: P450, Cytochrome P450; HPLC, high performance liquid chromatography; LC/MS, liquid chromatography/mass spectrometry; HLM, human liver microsome; ITZ, itraconazole; OH-ITZ, hydroxy-itraconazole CYP3A4+b₅, CYP3A4 with co-expressed cytochrome b₅; CYP3A5+b₅, CYP3A5 with co-expressed cytochrome b₅; IUL, Indiana University Liver Bank

Abstract

Vinorelbine is a semi-synthetic vinca alkaloid used in the treatment of advanced breast and non-small cell lung cancers. Vincristine, a related vinca alkaloid, is 9-fold more efficiently metabolized by CYP3A5 than by CYP3A4 *in vitro*. This study quantified the relative contribution of CYP3A4 and CYP3A5 to the metabolism of vinorelbine *in vitro* using cDNA-expressed human P450s and human liver microsomes (HLMs). CYP3A4 and CYP3A5 were identified as the P450s capable of oxidizing vinorelbine using a panel of human enzymes and selective P450 inhibitors in HLMs. For CYP3A4 co-expressed with cytochrome b₅ (CYP3A4+b₅) and CYP3A5+b₅, the Michaelis-Menten constants for vinorelbine were 2.6 μ M and 3.6 μ M, respectively, but the V_{max} of 1.4 pmol/min/pmol was common to both enzymes. In HLMs the intrinsic clearance of vinorelbine metabolism was highly correlated with CYP3A4 activity and there was no significant difference in intrinsic clearance between CYP3A5 high and low expressers. Using radiolabeled vinorelbine substrate there were clear qualitative differences in metabolite formation fingerprints between CYP3A4+b₅ and CYP3A5+b₅ as determined by NMR and MS analysis. One major metabolite (M2), a didehydro-vinorelbine, was present in both recombinant and microsomal systems but was more abundant in CYP3A4+b₅ incubations. We conclude that despite the equivalent efficiency of recombinant CYP3A4 and CYP3A5 in vinorelbine metabolism, the polymorphic expression of CYP3A5, as shown by the kinetics with HLMs, may have a minimal effect on systemic clearance of vinorelbine.

Introduction

Vinorelbine is a semi-synthetic vinca alkaloid used as chemotherapy primarily in the treatment of advanced breast and non-small-cell lung cancers (NSCLC). The advantages of vinorelbine over the naturally occurring vinca alkaloids, such as vincristine, include less overall drug-related toxicity due to a lower therapeutic dose (4 to 10-fold) and a broader anti-tumor spectrum (Leveque and Jehl, 1996).

Clinical pharmacokinetic studies of vinorelbine reveal significant interpatient variability (Gauvin, et al., 2002, Gauvin, et al., 2002, Qian, et al., 2011). Wong et al. reported no association of vinorelbine pharmacokinetic parameters with *ABCB1* or *CYP3A5* genotypes; however, the study was not adequately powered to truly evaluate for genetic. Furthermore, this study found an association between patient body surface area and myelosuppression; however, they found no association of either of these factors with vinorelbine pharmacokinetics (Wong, et al., 2006). As such, while there are a number of factors that may be contributing to the significant variability in vinorelbine pharmacokinetics (Baker and Sparreboom, 2006, Wong, et al., 2006), one that remains to be systematically investigated is the potential impact of variability of genes encoding important drug metabolizing enzymes on vinorelbine pharmacokinetics. Cytochrome P450 enzymes are a superfamily of hemoproteins responsible for most oxidative metabolic drug clearance in vivo, including metabolism of the vinca alkaloids. The CYP3A family includes CYP3A4, which alone comprises over 30% of hepatic enzymes and is involved in the metabolism for over 50% of marketed drugs that rely on metabolic elimination. CYP3A5 is structurally similar to CYP3A4, yet the substrate selectivity of these highly homologous proteins differs unpredictably (Kuehl, et al., 2001, Lamba, et al., 2002, Xie HG, 2004). Genetic polymorphisms of *CYP3A5* affect protein expression and activity, and consequently alter the intrinsic clearances of drugs selectively metabolized by CYP3A5 (Kuehl, et al., 2001, Lamba, et

al., 2002, Xie HG, 2004). Subjects homozygous or heterozygous for the *CYP3A5**1 allele are characteristically high expressers of the functional protein (Kuehl, et al., 2001) whereas the *CYP3A5**3, *6, and *7 alleles result in greatly diminished expression of the enzyme (Hustert, et al., 2001, Kuehl, et al., 2001, Lamba, et al., 2002, Xie HG, 2004). *CYP3A5* is expressed by approximately 55% of African-Americans but only 10-20% of Caucasians (Kuehl, et al., 2001, Roy, et al., 2005).

Vincristine, a related vinca alkaloid, is metabolized by cytochrome P450 (CYP) 3A enzymes, *CYP3A4* and *CYP3A5* (Dennison, et al., 2006). Vincristine is highly selectively metabolized by *CYP3A5* in vitro, suggesting the possible need for an individualized therapeutic approach (Dennison, et al., 2006). It is well established that African-Americans have poorer overall survival rates compared to Caucasians in a number of malignancies for which vincristine is a core chemotherapeutic agent (Longo, et al., 1986, Pollock, et al., 2000). Individuals that express *CYP3A5* may metabolize vincristine more efficiently than non-expressers, resulting in lower vincristine exposure and thus potentially less drug efficacy and toxicity. Clinical data demonstrate less vincristine-induced peripheral neuropathy in African-Americans, and a recent retrospective study in children diagnosed with ALL and treated with vincristine positively correlated increased neuropathy in *CYP3A5* non-expressers (Egbelakin, et al., 2011, Renbarger, et al., 2007).

Vinorelbine, as a member of the vinca alkaloid family, could be hypothesized to be similar to vincristine in the contribution of *CYP3A5*-mediated metabolism with analogous clinical outcomes. A study using human liver microsomes with known P450 enzyme protein concentrations suggested that vinorelbine is extensively metabolized by *CYP3A4* but not by *CYP2D6*; the role of *CYP3A5* was not clearly defined (Beulz-Riche, et al., 2005).

Preliminary retrospective clinical studies have explored the possible association between *CYP3A5* genotype and clinical response to vinorelbine. Wong et.al only found a weak correlation between vinorelbine clearance and both *CYP3A5* expression status and a common *ABCB1* genotype (Wong, et al., 2006). In a study with NSCLC patients, presence of a *CYP3A5*1* allele was found to correlate to a slightly higher overall chemotherapy response to vinorelbine (Pan, et al., 2008). To clarify the effect of *CYP3A5* expression, we quantified the relative contribution of *CYP3A4* and *CYP4A5* to the metabolic clearance of vinorelbine in vitro and used MS/MS and NMR to identify the major oxidative metabolites specific to *CYP3A4*.

Materials and Methods

Chemicals and Enzymes

Vinorelbine tartrate, ketoconazole, omeprazole, quinidine, trimethoprim, sulfaphenazole, α -naphthoflavone, pilocarpine, diethyldithiocarbamate, thioTEPA and NADPH were purchased from Sigma-Aldrich (St. Louis, MO). Vinorelbine [$^3\text{H}(\text{G})$] (5 Ci/mmol) was obtained from American Radiolabeled Chemicals, Inc. (St. Louis, MO). All other reagents were of HPLC grade and were purchased from Fisher Scientific (Pittsburg, PA).

Supersomes containing cDNA-expressed cytochrome P450s co-expressed with cytochrome P450-reductase with (*CYP1A1*, *1A2*, *2B6*, *2C19*, *2D6*, *2J2*, *3A4*, *3A5*, *3A7*, and *4A11*) and without (*CYP2A6*, *2C8*, *2C9*, and *2E1*) co-expressed cytochrome b_5 were purchased from the BD Gentest (Woburn, MA). The manufacturer provided the cytochrome P450-reductase activities, protein concentrations, and the cytochrome P450 content of the Supersomes.

Incubations with cDNA-Expressed Cytochrome P450s

Preliminary experiments with cDNA-expressed CYP3A4+b₅ and CYP3A5+b₅ significantly depleted the parent drug but did not result in quantifiable metabolite formation using HPLC with UV detection at a 1 μ M substrate concentration. Consequently, in all subsequent experiments, the rates of vinorelbine metabolism were quantified by substrate depletion. Linearity of time and protein content was used to determine incubation conditions suitable for all substrate concentrations, and percent vinorelbine depletion ranged from 8 to 33 % from initial concentrations as determined from the –NADPH controls; statistical significance between samples and –NADPH controls was determined. Less than 5 % day-to-day variability was observed in HPLC-UV analysis as compared to QC controls, and the limit of quantification of vinorelbine was 0.1 μ M.

Incubations were performed under conditions previously developed to study the oxidation of vincristine (Dennison, et al., 2006). Samples were incubated in an oscillating water bath at 37°C for specified time as determined per experiment. Vinorelbine in methanol (MeOH) was added to each 3 mL polypropylene reaction vial and evaporated to dryness in a centrifuge under vacuum prior to all incubations (Thermo Electron Corporation Savant, SC210A SpeedVac Concentrator). Two hundred microliters of 100 mM Na₂HPO₄ buffer with 5 mM MgCl₂, pH 7.4, was added to each vial and vortexed to ensure the drug was in solution prior to incubation. Each vial was placed in the 37°C water bath and pre-incubated for 3 min. Enzyme was then added, followed by NADPH after a further 3 min to start the reaction. To terminate the reaction, an equal volume (200 μ L) of acetonitrile (ACN) was added to each vial at the appropriate time to quench the incubation. Vials were immediately placed on ice and the internal standard, ketoconazole (1 μ M in MeOH) was added. Samples were then placed into a -80°C freezer for a minimum of 30 min, then subsequently thawed and centrifuged for 10 min (3000 x rpm, 20°C) to

precipitate any excess salt. The clear liquid was collected and stored at -80°C until HPLC analysis.

A panel of fourteen human drug metabolizing, cDNA-expressed P450s (1A1, 1A2, 2B6, 2C19, 2D6, 2J2, 3A4, 3A5, 3A7, 4A11, 2A6, 2C8, 2C9, and 2E1) were incubated with $1\text{ }\mu\text{M}$ vinorelbine and 30 pmol/mL of each enzyme for 12 min in duplicate. Control reactions did not contain NADPH.

To determine the Michaelis-Menten parameters of vinorelbine for CYP3A4+b₅ and CYP3A5+b₅, incubations were performed in triplicate at six vinorelbine concentrations of 1, 2, 3, 5, 7, and $10\text{ }\mu\text{M}$. Incubation controls were also performed in triplicate and lacked NADPH. Non-incubated controls consisted of vinorelbine in buffer. Samples were incubated with 30 pmol/mL of recombinant enzyme for 5 min. Concentrations for each sample were measured after a 5 min incubation, however as there was no metabolism observed in the –NADPH control samples, -NADPH controls were also used to indicate initial substrate concentrations at each time point. The rate of vinorelbine metabolism was calculated for each supersome from the pmol of parent drug lost per min per pmol of CYP3A4+b₅ or CYP3A5+b₅. Substrate concentrations were corrected for depletion using the –NADPH controls at each respective concentration as a 0 min time point concentration before calculating Michaelis-Menten parameters of vinorelbine metabolism. Corrected substrate concentrations were calculated as the average vinorelbine concentration over 5 min.

Incubations with Human Liver Microsomes (HLMs)

HLMs ($n = 56$) were prepared from human liver tissues from the Indiana University (IU) Liver Bank (Indiana University, Indianapolis, IN) as described previously (Gorski, et al., 1998). Each HLM was prepared from tissue that had been genotyped for *CYP3A5*, *3, *6, and *7 as

described in detail previously (Dennison, et al., 2007). Microsomal protein concentrations and CYP3A4 and CYP3A5 abundances of the HLMs were reported previously (Leveque and Jehl, 1996). From this bank of 56 livers, 20 were chosen to cover a broad range of CYP3A4 and CYP3A5 contents. Protein contents of the enzymes per HLM were quantified by Western blot (Dennison, et al., 2007). The activity of CYP3A4 was quantified from the rates of itraconazole hydroxylation and testosterone 6 β -hydroxylation; CYP3A5 activity was quantified by vincristine M1 formation rate (Dennison, et al., 2007). The formation rate of 6 β -hydroxylation from testosterone has been shown to be 27-fold faster by CYP3A4 than CYP3A5, suggesting that 6 β -hydroxylation formation could be used to determine CYP3A4 activity in HLMs (Leeder, et al., 2005). Likewise, OH-itraconazole formation has been previously shown to be CYP3A4 but not CYP3A5-mediated in supersomes (Isoherranen, et al., 2004). The 20 HLMs were incubated with 1 μ M vinorelbine with 0.8 mg/mL of protein for 12 min as described above. Each sample was run in triplicate and controls were incubated without NADPH addition. The rate of vinorelbine depletion (and metabolism) was calculated for each HLM from the pmoles of parent drug lost per min per mg of microsomal protein. Sample preparation was as described above.

HLM Incubations using Selective CYP450 Inhibitors

A pool of HLMs was incubated with vinorelbine and selective inhibitors of CYP450s above K_i concentrations as previously described to determine contributions of the major human drug metabolizing P450s to vinorelbine metabolism (Dennison, et al., 2007). Vinorelbine at 1 μ M was incubated with omeprazole (CYP2C19; 10 μ M), quinidine (CYP2D6; 1 μ M), trimethoprim (CYP2C8; 50 μ M), sulfaphenazole (CYP2C9; 10 μ M), ketoconazole (CYP3A; 1 μ M), α -naphthoflavone (CYP1A2; 1 μ M), pilocarpine (CYP2A6; 50 μ M), diethyldithiocarbamate (CYP2E1; 50 μ M), and thioTEPA (CYP2B6; 50 μ M) for 12 min (Bapiro,

et al., 2001, Dennison, et al., 2007, Rodrigues, 1999) with 0.8 mg/mL of protein from pooled HLMs. The HLM pool consisted of 5 livers pooled to be equally represented on the basis of total microsomal protein concentration; two of the five HLMs contained high concentrations of CYP3A5. Each incubation was run in triplicate and compared to controls that lacked inhibitor or both inhibitor and NADPH. Sample preparation was as described above.

Selective Inhibition of CYP3A4-Mediated Metabolism of Vinorelbine by Cyclosporine A in Supersomes and HLMs

Recombinant CYP3A4+b₅ and CYP3A5+b₅ were incubated with vinorelbine and Cyclosporine A (CsA) to confirm selectivity of CYP3A4 versus CYP3A5-mediated vinorelbine metabolism. Two human liver microsomes with similarly high CYP3A4 activities (> 50% drug depletion under incubation conditions of 0.16 mg HLM protein and 1 μ M vinorelbine for 12 min) were selected for this inhibition study. An HLM with high CYP3A5 protein content (IUL-73) and one with low protein content (IUL-55) were incubated in triplicate with vinorelbine and 25 μ M CsA at 0.3% MeOH (v/v). Controls contained 0.3% MeOH (v/v) and no CsA. Samples were incubated with 1 μ M vinorelbine for 12 min with either 30 pmol/mL of recombinant enzyme or 0.16 mg HLM protein.

High Pressure Liquid Chromatography Analysis

High Pressure Liquid Chromatography (HPLC) was used to quantify parent drug depletion and metabolite formation. The HPLC system consisted of a high pressure gradient binary pump and autosampler (1100 series, Agilent Technologies, Wilmington, DE) and an ultraviolet (UV) absorbance detector (1050 series, Hewlett Packard, Wilmington, DE). Post-incubation samples (as described above) were diluted with an equal volume of 0.2% formic acid and injected onto a reverse phase column (C₁₈ column, Inertsil ODS3, 3.0 x 150 mm, 5- μ m

particle size; MetaChem Technologies Inc., Torrance, CA). The mobile phases A and B consisted of 0.2% formic acid in MeOH with ratios of 80:20 and 20:80, respectively, flowing at a rate of 0.4 mL/min. A linear gradient over 25 min was used for simple drug depletion quantification: 0 min/0% B, 20 min/100% B, 20.1 min/0% B. A longer linear gradient over 75 min was used to distinguish metabolites formed: 0 min/0% B, 7 min/0% B, 57.1 min/70% B, 57.2 min/100% B, 67.2 min/100% B, 67.3 min/0% B. The parent drug, metabolites, and internal standard were detected by UV absorbance at a wavelength of 254 nm.

Radiolabeled Metabolite Analysis

Generally tritiated vinorelbine was purified using a HPLC no more than a day before incubations. ^3H vinorelbine (2×10^6 dpm; $0.9 \mu\text{M} + 5 \mu\text{M}$ cold vinorelbine) was incubated for 40 min with recombinant CYP3A4+b₅ and CYP3A5+b₅ enzymes (100 pmol/mL), and for 20 min with IU Liver (IUL)-73 (0.5 mg, high CYP3A5 protein content) and IUL-55 (0.5 mg, low CYP3A5 protein content). Incubation time and enzyme content were chosen to ensure extensive metabolite formation. Samples were injected neat and manually onto the HPLC aliquots of eluant were collected every 20 seconds into 7 mL scintillation vials. Scintillation fluid was added for a total volume of approximately 5 mL. Radioactive disintegrations per min (DPMs) were quantified using a liquid scintillation counter (Tri-Carb 2100TR, Packard Instrument Company, Meriden, CT) with quench correction.

Metabolite Identification

Metabolite structures were identified using LC/MS/MS and NMR analysis as described previously (Dennison, et al., 2006). Vinorelbine metabolites formed by CYP3A4+b₅ were isolated using a C₁₈ column (Phenomenex 150 x 4.60 mm, 5- μm particle size; Phenomenex, Inc., Torrance, CA). NMR samples were dissolved in ~150 μL of DMSO-*d*₆ and transferred to a

Wilma 335 NMR tube. Data were acquired on a Varian INOVA 500 NMR spectrometer with a Varian gradient, triple-resonance Cold Probe. The suite of experiments included a standard proton, 2D homonuclear gCOSY and TOCSY, direct-correlation multiplicity-edited HSQCAD, and long-range gHMBCAD. Water suppression for all experiments was accomplished with the wet1D element at the beginning of each pulse sequence. Data were acquired at 25°C and referenced to the solvent at 2.49 ppm for ^1H and 39.5 ppm for ^{13}C .

Data Analyses

Michaelis-Menten constants (K_M) and maximal rates of metabolism (V_{\max}) for each enzyme were determined by fitting the data with nonlinear least squares regression (WinNonlin 4.0, Pharsight, Mountain View, CA). The intrinsic clearance (Cl_{int}) of vinorelbine for CYP3A4+b₅ and CYP3A5+b₅ was calculated (equation 1).

$$Cl_{\text{int}} = \frac{V_{\max}}{K_M} \quad \text{Equation 1}$$

The intrinsic clearance of vinorelbine (Cl_{int}) in HLMs was predicted from the individual intrinsic clearances of expressed CYP3A4+b₅ and CYP3A5+b₅ and the previously determined enzyme concentrations in each HLM (equation 2). This approach assumes that the only difference between cDNA expressed P450 and microsomal P450 is in abundance and was previously successful in the case of vincristine (Dennison, et al., 2007). The average CYP3A4 and CYP3A5 (expressers only) concentration was 51.89 ± 38.5 pmol/mg and 29.05 ± 24.7 pmol/mg, respectively (Dennison et. al., 2007).

$$Cl_{\text{int}} = \left(\frac{V_{\max, \text{CYP3A4}}}{K_m, \text{CYP3A4} + [S]} \right) * [\text{CYP3A4}] + \left(\frac{V_{\max, \text{CYP3A5}}}{K_m, \text{CYP3A5} + [S]} \right) * [\text{CYP3A5}] \quad (\text{Equation 2})$$

The specific contribution of CYP3A5 to the intrinsic clearance of vinorelbine was estimated by subtracting the CYP3A4 component using the relationship between CYP3A4 activity (OH-ITZ formation) and rate of vinorelbine metabolism in low expressers of CYP3A5

(Dennison, et al., 2007). The two-sided Student t-test using was used to compare the velocities of vinorelbine metabolism by supersomes and in microsomes that contained either high or low contents of CYP3A5. A p-value of < 0.05 was considered statistically significant.

Results

Determination of P450 Enzymes that Contribute to Vinorelbine Metabolism by Recombinant Enzymes and HLMs:

Incubations with a panel of CYP450s (Figure 1A) indicated that vinorelbine was selectively metabolized by CYP3A4+b₅ (43.9% depletion) and CYP3A5+b₅ (43.6% depletion).

A pooled set of HLMs was incubated with vinorelbine (1 μ M) and selective P450 inhibitors to determine contribution of each enzyme to vinorelbine metabolism (Figure 2B). The percent remaining relative to no inhibitor control was: omeprazole, 89.6% (CYP2C19; 10 μ M); quinidine, 99.1% (CYP2D6; 1 μ M); trimethoprim, 94.4% (CYP2C8; 50 μ M); sulfaphenazole, 117.5 % (CYP2C9; 10 μ M); ketoconazole, 5.1 % (CYP3A4/5; 1 μ M); α -naphthoflavone, 96.5 % (CYP1A2; 1 μ M); pilocarpine, 94.5 % (CYP2A6; 50 μ M); diethyldithiocarbamate, 102.4 % (CYP2E1; 50 μ M); thioTEPA = 108.0 % (CYP2B6; 50 μ M). These data are consistent with the cDNA-expressed enzyme panel and indicate that only CYP3A enzymes are involved in vinorelbine microsomal oxidation.

CsA (25 μ M) inhibited > 80 % of CYP3A4-mediated vinorelbine metabolism but only 20 % of CYP3A5-mediated vinorelbine metabolism in supersomes (Figure 1C). This data indicates that CsA (25 μ M) can be used to selectively inhibit CYP3A4-mediated vinorelbine metabolism in HLMs. There was no difference in vinorelbine depletion in HLMs with comparable CYP3A4 but high (IUL-73) and low (IUL-55) CYP3A5 contents (26 % and 28 % remaining activity compared to no-inhibitor controls, respectively) (Figure 1C).

Determination of Michaelis-Menten Parameters of Vinorelbine Metabolism by Recombinant CYP3A4 and CYP3A5:

Percent vinorelbine depleted at each substrate concentration point after incubating with CYP3A4+b₅ and CYP3A5+b₅ supersomes was significantly different compared to –NADPH controls (Supplemental Table 1). CYP3A4+b₅ and CYP3A5+b₅ were found to have low K_m values (CYP3A4 2.63 ± 0.48 μM, CYP3A5 3.64 ± 0.96 μM) and similar V_{max} values (CYP3A4 1.37 ± 0.09 pmol VRL/min/pmol P450, CYP3A5 1.40 ± 0.15 pmol VRL/min/pmol P450) (Figure 2A, B, Table 1). The corresponding intrinsic clearances were 0.52 ± 0.06 μl/min/pmol CYP and 0.38 ± 0.06 μl/min/pmol P450 for CYP3A4 and CYP3A5 respectively (Table 1). The K_m, V_{max}, and Cl_{int} vinorelbine metabolism by CYP3A4 and CYP3A5 did not significantly differ (p > 0.05 for each parameter).

In this study, the presence of co-expressed cytochrome b₅ greatly increased the overall rate of vinorelbine depletion. When incubated with vinorelbine, CYP3A5 without cytochrome b₅ metabolized the parent at one-third of the rate of CYP3A5+b₅; CYP3A4 without cytochrome b₅ did not detectibly metabolize vinorelbine (data not shown).

Vinorelbine Metabolism in Human Liver Microsomes Expressing High and Low CYP3A5

Content:

To determine the relative contributions of CYP3A4 and CYP3A5 to the metabolism of vinorelbine, HLMS (n = 20) previously characterized for CYP3A activities were incubated with vinorelbine. There was positive association between the rate of vinorelbine depletion (pmol vinorelbine depletion/min/mg protein) and two highly selective CYP3A4 activities, itraconazole hydroxylation (r² = 0.93, ***p < 0.001) and testosterone 6β-hydroxylation (r² = 0.78, ***p < 0.001) as shown (Figures 3A and B). The rate of vinorelbine depletion was highly correlated (r²

= 0.89, *** $p < 0.001$) with the rate of vincristine M1 formation in CYP3A5 low expressers (Figure 3D) but these activities were weakly correlated ($r^2 = 0.23$, $p = 0.224$) in high CYP3A5 expressers in which both CYP3A4 and CYP3A5 contribute to vincristine M1 formation (Figure 3C). This correlation analysis indicates that in HLMs, CYP3A4 is primary enzyme responsible for the depletion of vinorelbine.

Predicted Hepatic Clearance of Vinorelbine:

The observed mean (\pm sd) rate of vinorelbine depletion by CYP3A5 high expressers (31.0 ± 18.7 pmol VRL/min/mg HLM) and low expressers (31.7 ± 18.9 pmol VRL/min/mg HLM) were not statistically different ($p = 0.941$; Table 2). The corresponding Cl_{int} values (after accounting for total microsomal protein in a 70 kg man) were 2546.7 ± 1534.2 mL/min and 2599.9 ± 1548.2 mL/min for CYP3A5 high expressers and low expressers, respectively. The relationship between the intrinsic clearance of vinorelbine depletion and itraconazole hydroxylation in low expressers was used to determine the contribution of CYP3A5 to vinorelbine intrinsic clearance in high expressers as previously described for vincristine (Figure 4; (Dennison, et al., 2007)). The clearance of vinorelbine depletion by CYP3A5 after correcting for CYP3A4 contribution was 2.5 ± 4.7 (μ L/min/mg protein) in high expressers and this was not significantly different to zero ($p = 0.27$).

Predicted rates of vinorelbine depletion in the HLMs were calculated using the additive Cl_{int} model for cDNA-expressed CYP3A4+b₅ and CYP3A5+b₅ (Equation 2) and were found to be 1.3-fold higher for the CYP3A5 high expressers (high, 27.4 ± 19.9 pmol VRL/min/mg HLM; low, 20.6 ± 15.2 pmol VRL/min/mg HLM) but not significantly different ($p = 0.428$) (Table 2). Predicted clearance using the cDNA-expressed enzyme Michaelis-Menten parameters over-

predicted the contribution of CYP3A5 (predicted to be 36 % higher than low CYP3A5-expressing HLMs) to the metabolism of vinorelbine in HLMs.

Radiolabeled Metabolite Detection:

Recombinant enzymes CYP3A4+b₅, CYP3A5+b₅, and an insect control were incubated with ³H vinorelbine to detect metabolites by liquid scintillation count. Three common metabolites were detected after incubations with recombinant enzymes CYP3A4 and CYP3A5. Metabolite 2 (M2) (Figure 6A, 6B) was the most prevalent (as identified by HPLC/MS/MS). In the radio-chromatogram depicting metabolism by CYP3A5 (Figure 6B), M2 had a 3-fold lower peak area (dpm) than for CYP3A4 (Figure 6A). However, the overall depletion of ³H vinorelbine was similar for both (CYP3A4= 69.4%, CYP3A5= 71.2%), perhaps suggesting that subsequent metabolism of M2 by CYP3A5 may be occurring.

Two HLMs were incubated with ³H vinorelbine, both with similarly high CYP3A4 activity and different CYP3A5 protein contents: IUL-55 (minimal CYP3A5 content, Figure 7A) and IUL-73 (high CYP3A5 content, Figure 7B). The control was IUL-73 lacking NADPH (Figure 7C). The overall depletion of ³H vinorelbine was similar for both (IUL-55 = 59.4%, IUL-73 = 64.1%), consistent with predominant metabolism of vinorelbine by CYP3A4. In the radio-chromatogram depicting vinorelbine metabolism by IUL-55, the M2 peak was 1.5 fold larger than that of the M2 peak formed with IUL-73, similar to the higher ratio of M2 detected within the CYP3A4 versus CYP3A5 supersomes.

Metabolite Structure Identification:

Metabolite structures were identified using MS/MS and NMR analysis. The structures of vinorelbine and the proposed metabolite structures are shown in Table 3 along with the product ions and description of the key product ions for vinorelbine. The N-oxide of vinorelbine, M1,

was determined from the NMR data. Significant downfield shifts to the carbons adjacent to N4', compared to parent, clearly indicate the presence of an N-oxide. M1, however, is thought to be a by-product of the extraction method, as it was not detected when the incubated sample supernatants were analyzed without additional sample preparation.

The main metabolite of interest, M2, was present in both the recombinant and microsomal systems. M2 has been identified as a didehydro metabolite. Based on its protonated molecular ion at m/z 777 and its MS/MS and NMR data, the additional double bond is on the tetrahydropyridyl ring of the 'catharanthine like' side of the molecule. Key MS/MS product ions used to support the structure included m/z 321, consistent with 'catharanthine like' side minus two hydrogens and m/z 469, consistent with no change to the vindoline side of the molecule. The resultant double bond could only exist in one of three places; between C3'-C14', C14'-C17', and C19'-C18'. Although, the exact location of this double bond could not be determined, the 18'-19' ethyl moiety is clearly observed in the NMR data, indicating that the dehydration occurred with C14' and an adjacent carbon.

Other more minor metabolites were tentatively identified from their MS/MS product ion data and their proposed structures are shown in Table 3. From the MS/MS data, oxidation occurred on both the vinorelbine and 'catharanthine like' side of the molecule. Oxidative demethylation was also observed on the vinorelbine moiety.

Discussion

In this study we tested the hypothesis that vinorelbine would be more efficiently metabolized by CYP3A5 than CYP3A4 in view of the finding that a related compound, vincristine, displayed this unusual selectivity. Similar to vincristine metabolism, only cDNA-

expressed CYP3A4 and CYP3A5 were able to metabolize vinorelbine. A library of highly selective P450 inhibitors confirmed that only CYP3A enzymes catalyzed the loss of vinorelbine from human liver microsomes. However, in contrast to vincristine metabolism, CYP3A5 did not selectively metabolize vinorelbine; the two CYP3A enzymes displayed similar efficiencies toward vinorelbine depletion in vitro. Therefore, CYP3A5 expression would not be predicted to affect systemic clearance of vinorelbine.

Consistent with this hypothesis, there was little difference in vinorelbine intrinsic clearance between the high expresser (*CYP3A5* *1/*1, *1/*3, *1/*6) and low expresser (*CYP3A5* *3/*3) genotype human liver microsomes. It is notable that two livers (IUL-57 and IUL-71) were found to be *1 carriers, which would be expected to be high expressers of CYP3A5 hepatic protein; however, these livers with both found to have low expression of CYP3A4 protein and as such were classified as low expressers. CYP3A5*1 carrier status was determined by process of elimination with testing for *3, *6, and *7 included. We anticipate two potential explanations for the low CYP3A5 protein expression in these livers, including: 1) an undetected genetic polymorphism for these cases that promoted loss of CYP3A5 protein expression or 2) perhaps the donors were in critical condition or chronically ill, thus resulting in altered protein production. The predicted human hepatic clearance was essentially the same in high expressers and low expressers. Correlation analysis also indicated that vinorelbine intrinsic clearance was highly associated with CYP3A4 activities in human liver microsomes but not CYP3A5 activity. This is consistent with the expectation that CYP3A5 genotype does significantly impact vinorelbine hepatic clearance.

Recombinant supersome incubations determined CYP3A4 and CYP3A5 to have similar K_M and V_{max} values for vinorelbine. Therefore, we hypothesized that microsomes expressing

CYP3A5 protein would have statistically higher drug depletion rates after normalization to CYP3A4 activity. However, despite protein levels of CYP3A5 accounting for 41% of total CYP3A content on average (in HLMs expressing CYP3A5), vinorelbine depletion in human liver microsomes was shown to be predominantly mediated by CYP3A4. Vinorelbine metabolism was inhibited to similar extents by CsA in HLMs with high and low CYP3A5 content and similar amounts of CYP3A4 protein (Figure 1C), suggesting that there was minimal contribution of CYP3A5 to vinorelbine metabolism in the high CYP3A5-expressing HLM.

Our recombinant enzyme data suggest that CYP3A5 may contribute if CYP3A5 protein levels are high enough in the liver. However, this in vitro prediction was probably not correct based on the HLM data. In HLMs with high CYP3A5 (in several cases higher than CYP3A4), the contribution of CYP3A5 was not detected. As such, we would conclude that the contribution of CYP3A5 is insignificant. Together, these data indicate that CYP3A5 expression may not play a clinically significant role in vinorelbine metabolism in vivo, unlike as previously shown with vincristine (Dennison, et al., 2006).

Based on the findings of this in vitro investigation, we would not expect vinorelbine metabolism to differ based on CYP3A5 genotype. Consistent with the results of our study, clinical data from Wong et al. support a lack of CYP3A5 contribution to clearance of vinorelbine (Wong, et al., 2006). In contrast, CYP3A5*1 genotype has even been shown to be moderately associated with better overall median survival rates in patients with NSCLC (Pan, et al., 2007). In the study of P450 genotypes and clinical outcomes in patients with NSCLC, they found that patients with at least one CYP3A5*1 allele had slower rates of tumor growth and a higher associated median survival rate than did patients without a CYP3A5*1 allele. As such, the patients in the two genotype groups in the NSCLC clinical trial would be expected to have

similar vinorelbine clearance rates. Any number of confounding factors could be contributing to therapeutic efficacy in CYP3A5*1 subjects. One possible explanation for the finding of this clinical trial is that there is an unidentified variable factor between the two genotype groups studied resulting in a difference in vinorelbine such as volume of distribution, active transport, or non-P450 parallel elimination pathways between groups resulting in greater vinorelbine exposure in the CYP3A5*1 genotype group. Another possible reason for the difference observed in this study is that CYP3A5 may be sequentially metabolizing an inactive vinorelbine metabolite that competes with vinorelbine at the level of the tumor, resulting in greater vinorelbine exposure at the level of the tumor. A noticeable difference between the metabolites formed by CYP3A4 and CYP3A5 was apparent when studying the radiochromatograms of metabolite profiles resulting from incubation of parent drug with individual recombinant enzymes. Metabolite 2 (M2) was observed when vinorelbine was incubated with both the recombinant and microsomal systems (Figures 6 and 7). However, formation of M2 was significantly lower in the presence of CYP3A5. In the recombinant enzyme system, M2 formation with CYP3A4 was 3-fold higher than with CYP3A5. The formation of M2 by IUL-55 (low CYP3A5 content) was 1.5-fold higher than by IUL-73 (high CYP3A5 content). By comparing the HLMs with similarly high CYP3A4 activity levels, it was assumed that a similar amount of M2 was formed by CYP3A4. A plausible hypothesis to address this discrepancy of M2 detection between systems expressing or not expressing CYP3A5 could be the sequential metabolism of M2 by CYP3A5.

In this study, tandem mass spectrometry analysis of *in vitro* incubations with both recombinant enzymes and human liver microsomes demonstrated M2 (didehydro-vinorelbine on the velbenamine side of the molecule) as the major vinorelbine metabolite formed by CYP3A4. This major metabolite of vinorelbine M2 is distinct from the major CYP3A-mediated metabolite

of vincristine M3, an unusual metabolite formed after an intramolecular amidation reaction (Dennison, et al., 2006). The molecular rearrangement of vincristine by CYP3A metabolism would not be expected for vinorelbine because of the chemical differences between the molecules on the catharanthine side.

As for other possible metabolites of vinorelbine, previous clinical studies of vinorelbine have shown the presence of the metabolite deacetyl-vinorelbine (deacetyl-navelbine) in the urine (Nicot, et al., 1990, Van Heugen, et al., 2001). However, deacetyl-vinorelbine has only been detected in trace amounts, representing only 0.25% of the vinorelbine dose (30 mg/m²). Although it has been detected in trace amounts *in vivo* within blood and feces (Leveque and Jehl, 1996, Van Heugen, et al., 2001), vinorelbine N-oxide in our study was determined to be a by-product of the extraction process (data not shown) and is therefore not thought to occur via CYP3A4-mediated oxidation. Recombinant CYP450s and HLMs are only responsible for oxidative metabolism of vinorelbine, so deacetyl-vinorelbine was not detected in this *in vitro* study. Recently, a number of vinorelbine metabolites, including vinorelbine N-oxide, were identified using LC-MS/MS from human biological fluids and categorized as being found in blood, urine, or faeces (de Graeve, et al., 2008). A comparison of the metabolites (M13, M7, M10, M5, M15, and M2) identified from human biological fluids (de Graeve, et al., 2008) showed strong similarities with metabolites M2, M3, M4, M6, M7, and M8, respectively (Table 3) identified in this study as being CYP3A4-mediated. These metabolites therefore may be biologically relevant, especially M2, because it was the predominant metabolite formed in human liver microsomes lacking CYP3A5.

In conclusion, based on our *in vitro* findings, CYP3A enzymes are predicted to metabolize vinorelbine, primarily to a didehydro-metabolite M2 (Table 3). However,

polymorphic CYP3A5 expression is not expected to significantly contribute to vinorelbine metabolism in vivo because unlike vincristine, vinorelbine is not selectively metabolized by CYP3A5.

Authorship Contributions

Participated in research design: Topletz, Dennison, Hall, Renbarger

Conducted Experiments: Topletz, Barbuch, Hadden

Contributed new reagents or analytical tools: Topletz, Barbuch, Hadden, Hall, Renbarger

Performed data analysis: Topletz, Barbuch, Hadden, Dennison, Hall, Renbarger

Wrote or contributed to the writing of the manuscript: Topletz, Dennison, Barbuch, Hall, Renbarger

References

- Baker SD and Sparreboom A (2006) Predicting vinorelbine disposition and toxicity: Does BSA provide more than a "bad statistical association"? *J Clin Oncol* 24: 2412-2413.
- Bapiro TE, Egnell AC, Hasler JA and Masimirembwa CM (2001) Application of higher throughput screening (hts) inhibition assays to evaluate the interaction of antiparasitic drugs with cytochrome p450s. *Drug Metab Dispos* 29: 30-35.
- Beulz-Riche D, Grude P, Puozzo C, Sautel F, Filaquier C, Riche C and Ratanasavanh D (2005) Characterization of human cytochrome p450 isoenzymes involved in the metabolism of vinorelbine. *Fundam Clin Pharmacol* 19: 545-553.
- de Graeve J, van Heugen JC, Zorza G, Fahy J and Puozzo C (2008) Metabolism pathway of vinorelbine (navelbine) in human: Characterisation of the metabolites by hplc-ms/ms. *J Pharm Biomed Anal* 47: 47-58.
- Dennison JB, Jones DR, Renbarger JL and Hall SD (2007) Effect of cyp3a5 expression on vincristine metabolism with human liver microsomes. *J Pharmacol Exp Ther* 321: 553-563.
- Dennison JB, Kulanthaivel P, Barbuch RJ, Renbarger JL, Ehlhardt WJ and Hall SD (2006) Selective metabolism of vincristine in vitro by cyp3a5. *Drug Metab Dispos* 34: 1317-1327.
- Egbelakin A, Ferguson MJ, MacGill EA, Lehmann AS, Topletz AR, Quinney SK, Li L, McCammack KC, Hall SD and Renbarger JL (2011) Increased risk of vincristine neurotoxicity associated with low cyp3a5 expression genotype in children with acute lymphoblastic leukemia. *Pediatr Blood Cancer* 56: 361-367.
- Gauvin A, Pinguet F, Culine S, Astre C, Cupissol D and Bressolle F (2002) Blood and plasma pharmacokinetics of vinorelbine in elderly patients with advanced metastatic cancer. *Cancer Chemother Pharmacol* 49: 48-56.
- Gauvin A, Pinguet F, Culine S, Astre C, Gomeni R and Bressolle F (2002) A limited-sampling strategy to estimate individual pharmacokinetic parameters of vinorelbine in elderly patients with advanced metastatic cancer. *Anticancer Drugs* 13: 473-480.
- Gorski J, Haehner B, Jones D, O'Mara E and Hall S (1998) The contribution of intestinal and hepatic cyp3a to the interaction between midazolam and clarithromycin. *Clinical Pharmacology and Therapeutics* 64: 133-148.
- Hustert E, Haberl M, Burk O, Wolbold R, He Y, Klein K, Nuessler A, Neuhaus P, Klattig J, Eiselt R, Koch I, Zibat A, Brockmoller J, Halpert J, Zanger U and Wojnowski L (2001) The genetic determinants of the cyp3a5 polymorphism. *Pharmacogenetics* 11: 773-779.
- Isoherranen N, Kunze KL, Allen KE, Nelson WL and Thummel KE (2004) Role of itraconazole metabolites in cyp3a4 inhibition. *Drug Metab Dispos* 32: 1121-1131.

Kuehl P, Zhang J, Lin Y, Lamba J, Assem M, Schuetz J, Watkins P, Daly A, Wrighton S, Hall S, Maurel P, Relling M, Brimer C, Yasuda K, Venkataramanan R, Strom S, Thummel K, Boguski M and Schuetz E (2001) Sequence diversity in cyp3a promoters and characterization of the genetic basis of polymorphic cyp3a5 expression. *Nature Genetics* 27: 383-391.

Lamba J, Lin Y, Schuetz E and Thummel K (2002) Genetic contribution to variable human cyp3a-mediated metabolism. *Advanced Drug Delivery Reviews* 54: 1271-1294.

Leeder JS, Gaedigk R, Marcucci KA, Gaedigk A, Vyhldal CA, Schindel BP and Pearce RE (2005) Variability of cyp3a7 expression in human fetal liver. *J Pharmacol Exp Ther* 314: 626-635.

Leveque D and Jehl F (1996) Clinical pharmacokinetics of vinorelbine. *Clinical Pharmacokinetics* 31: 184-197.

Longo D, Young R, Wesley M, Hubbard S, Duffey P, Jaffe E and deVita V (1986) Twenty years of mopp therapy for hodgkin's disease. *Journal of Clinical Oncology* 4: 1295-1306.

Nicot G, Lachatre G, Marquet P, Bonnaud F, Vallette JP and Rocca JL (1990) High-performance liquid chromatographic determination of navelbine in human plasma and urine. *J Chromatogr* 528: 258-266.

Pan JH, Han JX, Wu JM, Sheng LJ and Huang HN (2007) Cyp450 polymorphisms predict clinic outcomes to vinorelbine-based chemotherapy in patients with non-small-cell lung cancer. *Acta Oncol* 46: 361-366.

Pan JH, Han JX, Wu JM, Sheng LJ, Huang HN and Yu QZ (2008) Mdr1 single nucleotide polymorphisms predict response to vinorelbine-based chemotherapy in patients with non-small cell lung cancer. *Respiration* 75: 380-385.

Pollock B, DeBaun M, Camitta B, Shuster J, Ravindranath Y, Pullen D, Land V, Mahoney DJ, Lauer S and Murphy S (2000) Racial differences in the survival of childhood b-precursor acute lymphoblastic leukemia: A pediatric oncology group study. *Journal of Clinical Oncology* 18: 813-823.

Qian J, Wang Y, Chang J, Zhang J, Wang J and Hu X (2011) Rapid and sensitive determination of vinorelbine in human plasma by liquid chromatography-tandem mass spectrometry and its pharmacokinetic application. *J Chromatogr B Analyt Technol Biomed Life Sci* 879: 662-668.

Renbarger JL, McCammack KC, Rouse CE and Hall SD (2007) Effect of race on vincristine-associated neurotoxicity in pediatric acute lymphoblastic leukemia patients. *Pediatr Blood Cancer*

Rodrigues AD (1999) Integrated cytochrome p450 reaction phenotyping: Attempting to bridge the gap between cdna-expressed cytochromes p450 and native human liver microsomes. *Biochem Pharmacol* 57: 465-480.

Roy JN, Lajoie J, Zijenah LS, Barama A, Poirier C, Ward BJ and Roger M (2005) Cyp3a5 genetic polymorphisms in different ethnic populations. *Drug Metab Dispos* 33: 884-887.

Van Heugen JC, De Graeve J, Zorza G and Puozzo C (2001) New sensitive liquid chromatography method coupled with tandem mass spectrometric detection for the clinical analysis of vinorelbine and its metabolites in blood, plasma, urine and faeces. *J Chromatogr A* 926: 11-20.

Wong M, Balleine RL, Blair EY, McLachlan AJ, Ackland SP, Garg MB, Evans S, Farlow D, Collins M, Rivory LP, Hoskins JM, Mann GJ, Clarke CL and Gurney H (2006) Predictors of vinorelbine pharmacokinetics and pharmacodynamics in patients with cancer. *J Clin Oncol* 24: 2448-2455.

Xie HG WA, Kim RB, Stein CM, Wilkinson GR (2004) Genetic variability in cyp3a5 and its possible consequences. *Pharmacogenomics* 5: 243-272.

Footnotes:

This work was supported by the National Institutes of Health National Center for Research Resources [K23 RR019956].

Legends for Figures

Figure 1: (A) Percent depletion from control for a panel of cytochrome P450 enzymes incubated with vinorelbine. Incubations were performed in duplicate, using 5 μ M vinorelbine and 200 pmol/mL of CYP450 for 60 min. Control was insect cell protein that did not express CYP450 enzymes. CYP3A4 and CYP3A5 were the only enzymes that showed statistically significant difference in vinorelbine depletion from the control ($***p < 0.001$). (B) Remaining percent active depletion of vinorelbine by human liver microsomes normalized to control after chemical inhibition by hepatic CYP450s. Vinorelbine (1 μ M) was incubated for 12 min with 0.8 mg/mL of protein from pooled human liver microsomes and each chemical inhibitor at their respective K_i concentrations. The control contained no chemical inhibitors. Only the inhibition of CYP3A by ketoconazole (1 μ M) showed significantly diminished activity ($***p < 0.001$). (C) Inhibition of vinorelbine metabolism by Cyclosporine A in CYP3A4 and CYP3A5 supersomes and HLMs with high CYP3A5 (IUL-73) and low CYP3A5 (IUL-55) expression.

Figure 2: (A) Vinorelbine depletion rate plotted against vinorelbine concentration when incubated with CYP3A4+b₅ (○) or CYP3A5+b₅ (●). (B) Eadie-Hofstee plots of CYP3A4+b₅ (○) or CYP3A5+b₅ (●)-mediated metabolism of vinorelbine. All incubations were performed in triplicate with 30 pmol/mL CYP3A4+b₅ or CYP3A5+b₅ for 5min. Lines represent the best fit to the Michaelis-Menten equation for vinorelbine metabolism by CYP3A4+b₅ (dotted line) or CYP3A5+b₅ (solid line) as determined using WinNonLin.

Figure 3: Relationships between rate of vinorelbine metabolism by human liver microsomes and the rates of OH-ITZ formation from itraconazole (4A; $r^2 = 0.93$, $***p < 0.001$), testosterone

6- β -hydroxylation (4B; $r^2 = 0.78$, $***p < 0.001$) and vincristine M1 formation in human liver microsomes with high CYP3A5 protein content (4C; $r^2 = 0.23$, $p = 0.224$) and low protein content (4D; $r^2 = 0.89$, $***p < 0.001$). Microsomes are designated by CYP3A5 protein content: high (●) and low (○). All incubations were performed in triplicate; 1 μ M vinorelbine and 0.8 mg/mL protein content per human liver microsome were incubated for 12 min.

Figure 4: Formation of OH-ITZ (μ L/min/mg protein) plotted against vinorelbine clearance (μ L/min/mg protein) between human liver microsomes with high (●) and low (○) CYP3A5 protein content. Regression line and 95% confidence intervals represent the correlation between HLMs with low CYP3A5 content (○), in which clearance is predominantly CYP3A4-mediated. The majority of HLMs regardless of CYP3A5 expression fell within the 95% confidence intervals. After correcting for CYP3A4 contribution, CYP3A5 did not significantly contribute to vinorelbine clearance in HLMs.

Figure 5: Radiochromatograms of 3 H vinorelbine (DPM; disintegrations per min) incubated with CYP3A4+b₅ (6A), CYP3A5+b₅ (6B), or non CYP450-expressing insect control (6C) supersomes. Fractions were separated by HPLC, collected in 20 second intervals, and quantified by scintillation count. The relative formation of M2 appears to be 3-fold higher when vinorelbine is incubated with CYP3A4+b₅ than with CYP3A5+b₅ (VRL = vinorelbine, M2 = metabolite 2).

Figure 6: Radiochromatograms of 3 H vinorelbine (DPM; disintegrations per min) incubated with human liver microsomes IUL-55 (low CYP3A5 protein content; 7A), IUL-73 (high

CYP3A5 protein content; 7B), or IUL-73 lacking NADPH as control (7C). Fractions were separated by HPLC, collected in 20 second intervals, and quantified by scintillation count. The relative detection of M2 is 1.5-fold higher for IUL-55 than by IUL-73 (VRL = vinorelbine, M2 = metabolite 2). Based upon supersome data, and that both IUL-55 and IUL-73 contained similar amounts of CYP3A4 protein, the difference in M2 detection may be due to subsequent metabolism of M2 by CYP3A5 in IUL-73.

Tables

Table 1: Michaelis-Menten parameters for vinorelbine metabolism by CYP3A4 and CYP3A5 supersomes.

	K_M (μM)	V_{max} (pmol VRL/min/pmol P450)	Cl_{int} (μL/min/pmol P450)
CYP3A4	2.63 ± 0.48	1.37 ± 0.09	0.52 ± 0.06
CYP3A5	3.64 ± 0.96	1.40 ± 0.15	0.38 ± 0.06

Table 2: Genotypes of HLMs and Vinorelbine Metabolism Rates

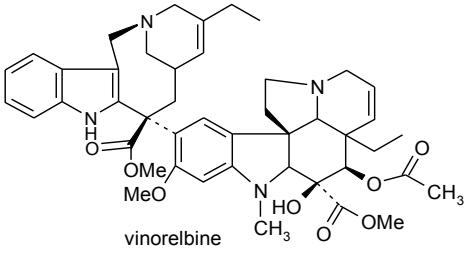
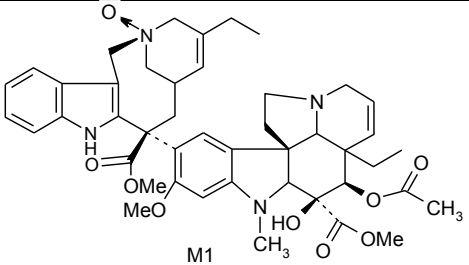
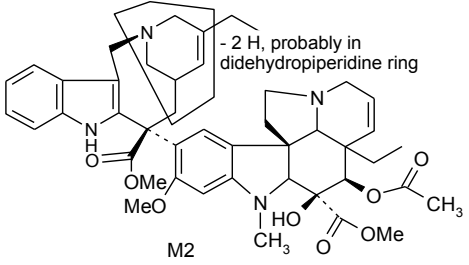
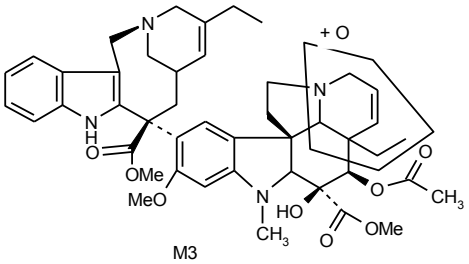
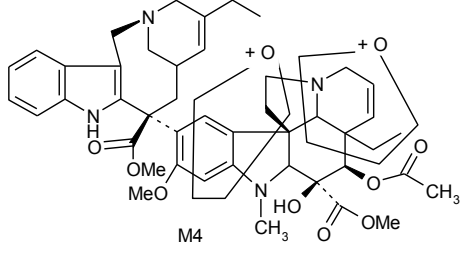
HLM	CYP3A5 Genotype ^a	Gender	CYP3A4 Protein Content (pmol/mg)	CYP3A5 Protein Content (pmol/mg)	$v_{[1\mu\text{M Vinorelbine}]}$ (pmol/min/mg)	Intrinsic Clearance ^b (mL/min)	Hepatic Clearance ^c (mL/min)
<i>CYP3A5 High Expressers:</i>							
IUL-40	*1/*1	M	103.8	89.4	48.2	3952.3	337.1
IUL-41	*1/*3	F	14.7	20.5	33.1	2716.9	249.2
IUL-42	*1/*3	F	23.7	16.1	17.2	1414.9	141.0
IUL-59	*1/*3	N/A	36.3	14.7	29.0	2379.3	222.8
IUL-66	*1/*3	M	24.4	20.6	24.4	1999.5	191.8
IUL-73	*1/*3	F	96.1	20.1	67.6	5546.3	433.7
IUL-74	*1/*6	F	10.7	26.2	11.2	915.4	94.4
IUL-85	*1/*3	M	85.5	24.8	17.7	1448.9	144.1
<i>CYP3A5 Low Expressers:</i>							
IUL-6	*3/*3	N/A	19.0	0.8	13.9	1137.1	115.5
IUL-49	*3/*3	M	48.8	0.8	28.9	2370.3	222.1
IUL-52	*3/*3	M	14.8	0.0	10.3	846.2	87.6
IUL-55	*3/*3	N/A	130.4	0.8	57.6	4722.5	385.8
IUL-57	*1/*3	M	40.6	0.8	19.5	1598.6	157.4
IUL-65	*3/*3	M	15.6	0.6	15.0	1232.8	124.4
IUL-71	*1/*7	F	10.9	1.1	16.7	1371.5	137.1
IUL-72	*3/*3	F	25.3	0.9	17.5	1434.7	142.8
IUL-75	*3/*3	N/A	78.2	2.3	46.2	3788.5	326.1
IUL-78	*3/*3	F	109.5	3.1	52.4	4296.9	359.4
IUL-81	*3/*3	M	71.7	2.0	40.8	3350.7	295.9
IUL-86	*3/*3	N/A	77.8	2.1	61.5	5049.2	405.3
			$v_{[1\mu\text{M Vinorelbine}]}$ (pmol/min/mg)		Intrinsic Clearance ^b (mL/min)	Hepatic Clearance ^c (mL/min)	
<i>Mean: CYP3A5 High Expressers:</i>			31.0 ± 18.7		2546.7 ± 1534.2	226.8 ± 112.4	
<i>Mean: CYP3A5 Low Expressers:</i>			31.7 ± 18.9		2599.9 ± 1548.2	229.9 ± 117.4	
<i>p-value</i>			0.941		0.941	0.952	

^a Genotypes and protein content (pmol/mg) of CYP3A4 and CYP3A5 per HLM from Dennison et. al, 2007.

^b Intrinsic clearance = $Cl_{\text{int}} = v_{[1\mu\text{M Vinorelbine}]} \cdot 1500 \text{ g liver} \cdot 45 \text{ mg microsomal protein/g liver} / K_m$ for a 70-kg man. (Dennison, et al., 2007)

^c Predicted hepatic clearance = $CL_H = Q \cdot (Cl_{\text{int}} \cdot f_u) / (Q + (Cl_{\text{int}} \cdot f_u))$, where $f_u = 0.11$ and $Q = 1.5 \text{ L/min}$ for a 70-kg man.

Table 3: Vinorelbine and its CYP3A4 metabolites based on LC/MS/MS and NMR data.

ID	M+H ⁺	MS/MS Product Ions	Proposed Metabolite Structure
Vinorelbine	779	719,701,510,469,457,323,122	 <p>vinorelbine</p>
M1	795	735,702,646,526, 469 ,457,339,202 ,138,122	 <p>M1</p>
M2	777	717,686,580,419,321,311	 <p>M2 - 2 H, probably in didehydropiperidine ring</p>
M3	795	735,717,674, 642 ,510.485,379,323 ,291,122	 <p>M3</p>
M4	811	526,508, 485 ,473,397,345,323,202	 <p>M4</p>

DMD #51094

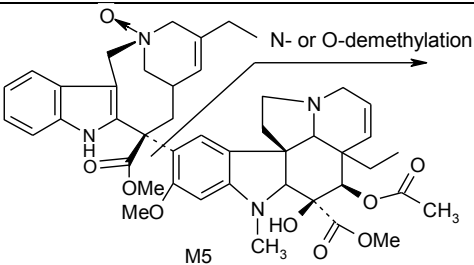
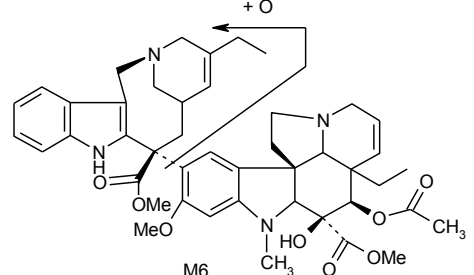
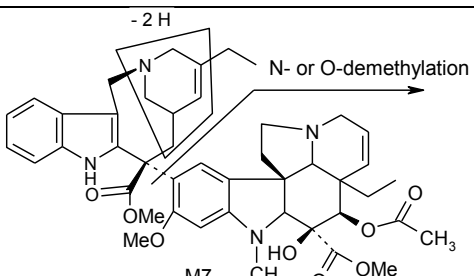
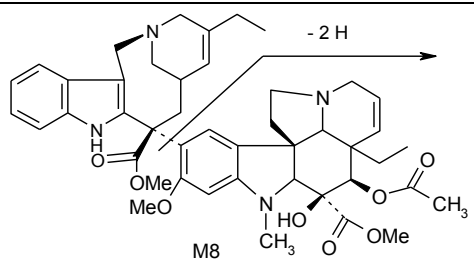
M5	781	610,455,443,138,122	 <p>M5</p>
M6	795	777,717,633,526,457,403,202,122 ,108	 <p>M6</p>
M7	763	704,672,566,535,455,423,321	 <p>M7</p>
M8	777	718,717,658,657,467,389	 <p>M8</p>

Figure 1

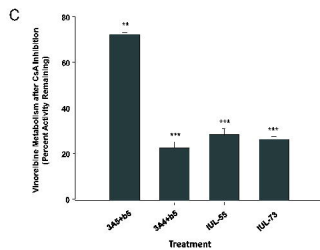
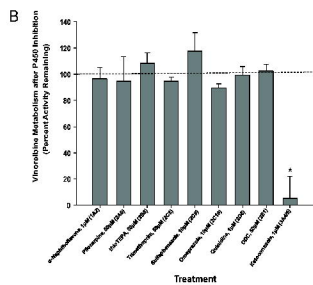
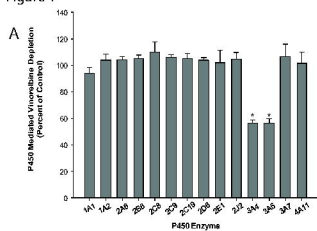
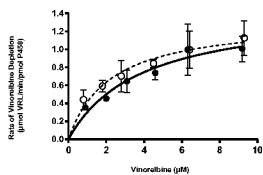


Figure 2

A



B

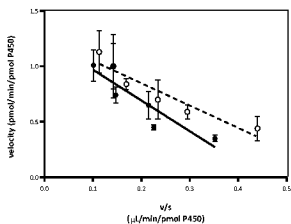


Figure 3

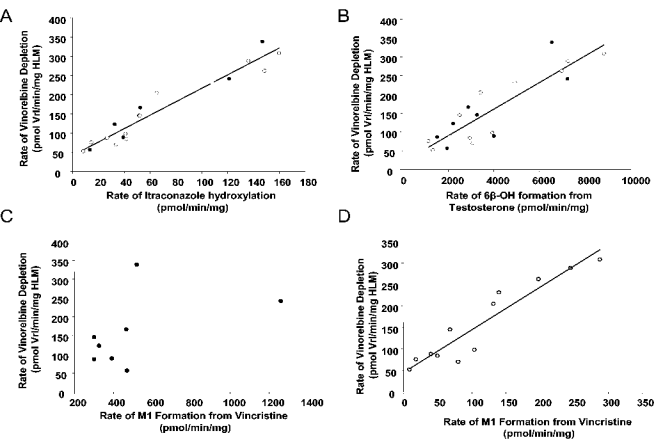


Figure 4

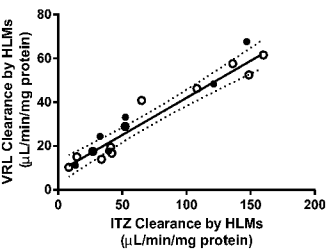


Figure 5

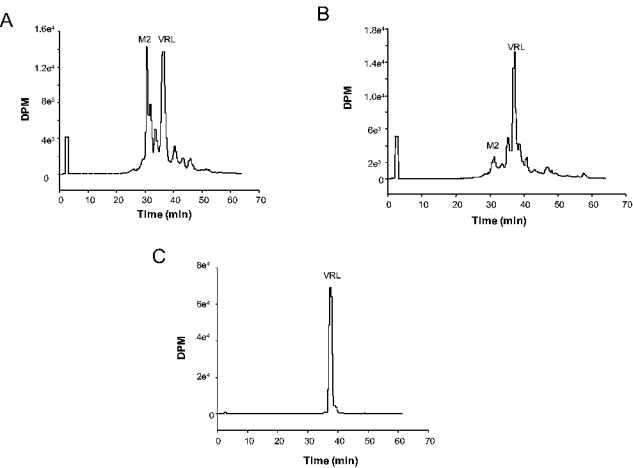
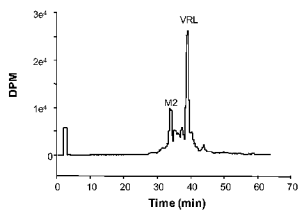
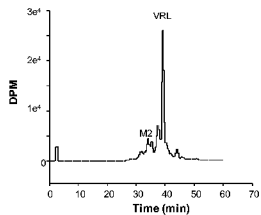


Figure 6

A



B



C

